Quantum Quench in One Dimension: Coherent Inhomogeneity Amplification and "Supersolitons"

Matthew S. Foster,[1,*] Emil A. Yuzbashyan,[1] and Boris L. Altshuler[2]
[1]Center for Materials Theory, Department of Physics and Astronomy, Rutgers University, Piscataway, New Jersey 08854, USA
[2]Physics Department, Columbia University, New York, New York 10027, USA
(Received 19 June 2010; published 23 September 2010)

We study a quantum quench in a 1D system possessing Luttinger liquid (LL) and Mott insulating ground states before and after the quench, respectively. We show that the quench induces power law amplification in time of any particle density inhomogeneity in the initial LL ground state. The scaling exponent is set by the fractionalization of the LL quasiparticle number relative to the insulator. As an illustration, we consider the traveling density waves launched from an initial localized density bump. While these waves exhibit a particular rigid shape, their amplitudes grow without bound.

DOI: 10.1103/PhysRevLett.105.135701 PACS numbers: 64.70.Tg, 05.45.Yv, 64.60.Ht, 67.85.−d

The shattering of cold glass in hot water is but one of many spectacular effects that can be induced by a rapid thermal quench in classical media. What happens when an isolated quantum phase of matter is subject to a sudden, violent deformation of its system Hamiltonian (a "quantum quench")? This question is now under vigorous investigation in cold atomic gases [1–4]. Long-time, out-of-equilibrium physics already observed in gases confined to one [2], two [3], and three [4] spatial dimensions includes oscillatory collapse and revival phenomena [2,4] and topological defect formation [3,5].

In this Letter, we study interaction quenches in one-dimensional (1D) quantum many body systems. Prior theory assuming spatially uniform dynamics has considered the postquench distribution of quasiparticles [6], correlation functions [7,8], thermalization [6,9], quantum critical scaling [10], etc. On the other hand, the stability of homogeneous solutions with respect to the spontaneous eruption of spatial nonuniformity is by no means guaranteed, due to the coupling between modes with different momenta and the extensive quantity of energy injected into the system by the quench. Indeed, homogeneous external perturbations are known to generate large spatial modulations in a variety of physical contexts [5,11]. We show here that quantum quenches can produce strongly inhomogeneous states via a mechanism that is ubiquitous in 1D.

We consider quenches across a quantum critical point, with initial (pre-) and final (postquench) Hamiltonians possessing Luttinger liquid (LL) and Mott insulator ground states, respectively. Specifically, we quench into the insulating phase of the quantum sine-Gordon model at the "Luther-Emery" (LE) point [8,10,12–14], where we are able to determine the dynamics analytically. The prequench ground state has an inhomogeneous density profile $\rho_0(x)$, which acts as a "seed" generating fluctuations in the space-time dynamics of local observables [15]. We find that an arbitrarily small deviation of $\rho_0(x)$ from a constant is dynamically amplified by the time evolution, see, e.g., Figs. 1 and 2. We argue that the mechanism responsible for the amplification is quasiparticle *fractionalization*, a generic attribute of gapless interacting particles in 1D [12,16]. We further illustrate the amplification effect for a localized (Gaussian) initial density "bump." This bump gives rise to a pair of nondispersive, noninteracting density waves that exhibit a rigid shape, with amplitudes that grow in time as a power law. We have dubbed these traveling density waves "supersolitons"; an example is depicted in Fig. 2.

Specifically, for the Fourier transform $\tilde{\rho}(t, k)$ of the density operator expectation value $\rho(t, x)$, we find the following exact asymptotic result, valid in the long time limit:

$$\frac{\tilde{\rho}(t,k)}{\tilde{\rho}_0(k)} = \cos(kt') - \mathcal{A}_\sigma(|k|t')^{\sigma/2}\cos\left(|k|t' + \frac{\pi\sigma}{4}\right). \quad (1)$$

Here $\mathcal{A}_\sigma$ is a nonuniversal, k-independent constant and $t' \equiv t/\bar{K}$, where $\bar{K} = 1/4$ locates the LE point (see below);

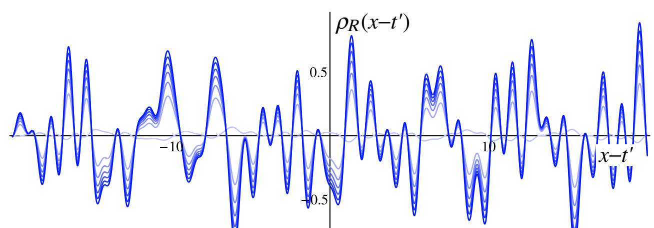

FIG. 1 (color online). Space-time evolution of the right-moving number density ρ_R after Luttinger liquid to Mott insulator quench, demonstrating the instability of spatially uniform dynamics; fainter (bolder) traces depict earlier (later) times. An infinitesimally small initial density inhomogeneity grows without bound. The figure is obtained from Eq. (1) with $\sigma = 0.8$, $\mathcal{A}_\sigma = 4.7$, and an initial density profile $\rho_0(x)$ given by a sum of 150 cosines with random amplitudes, phases, and wave numbers. Amplification occurs for any nonzero σ, corresponding to a nonzero fractionalization of the initial LL quasiparticles with respect to the insulator.

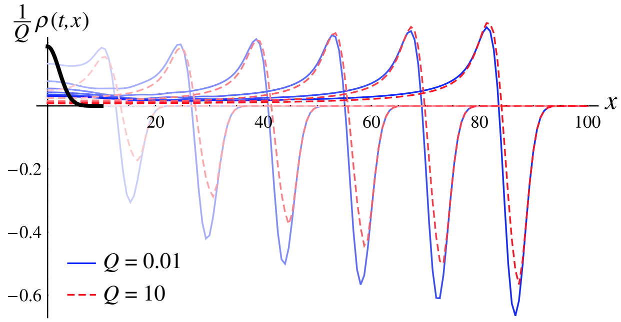

FIG. 2 (color online). The right-moving "supersoliton". The number density evolution after Luttinger liquid to Mott insulator quench is depicted as in Fig. 1, but here for a Gaussian initial profile $\sqrt{\pi}\Delta\rho_0(x) = Q\exp(-x^2/\Delta^2)$ (heavy black line), with $\sigma = 0.7$ and $\Delta = 3$, now obtained via numerical integration of the exact bosonization result [19]. Time series for two different Q are plotted; the densities are normalized relative to these. The evolution is reflection symmetric about $x = 0$.

the quench is performed at $t' = 0$. The exponent σ in Eq. (1) is determined by the relative fractionalization of the LL quasiparticle number with respect to the Mott insulator,

$$\sigma \equiv (\bar{K}/2K + K/2\bar{K}) - 1, \tag{2}$$

where K is the Luttinger parameter characterizing the initial Hamiltonian. Equation (1) implies that the density splits into nondispersing left- and right-moving components, $\rho(t,x) = \rho_R(x - t') + \rho_L(x + t')$. Interestingly, the long time response is linear in $\tilde{\rho}_0$ and enhanced at shorter wavelengths due to the fractional derivative ($|k|^{\sigma/2}$) factor. For $\sigma > 0$, the fluctuations of $\rho_{R,L}$ are continuously amplified by the quench, as demonstrated in Fig. 1.

In the rest of this Letter, we explain the setup and calculations leading to Eq. (1). Before the quench, our cold atom system is assumed to reside in the ground state $|0\rangle_{\rho_0}$ of the LL Hamiltonian

$$H_i = \int dx\left[\frac{vK}{2}\left(\frac{d\hat{\phi}}{dx}\right)^2 + \frac{v}{2K}\left(\frac{d\hat{\theta}}{dx}\right)^2 - \frac{\rho_0(x)}{q\sqrt{\pi}}\frac{d\hat{\theta}}{dx}\right], \tag{3}$$

where v is the sound velocity, K is the Luttinger parameter, and $\rho_0(x)/q$ is an external chemical potential, with $q \equiv K/v\pi$. The Hamiltonian in Eq. (3) governs the low-energy, long-wavelength physics of many gapless 1D cold atomic and condensed matter quantum systems [12,17]; in this Letter, we have in mind a 1D optical lattice gas of spin-polarized, neutral Fermi atoms, but other interpretations are possible. The short-ranged interatomic interactions determine v and K; repulsive (attractive) interactions correspond to $K < 1$ ($K > 1$), while the free Fermi gas has $K = 1$ and v equal to the bare Fermi velocity. The boson fields $\hat{\phi}$ and $\hat{\theta}$ encode fluctuations of the long-wavelength fermion number density $:\hat{\rho}:$ and current $:\hat{J}:$ on top of the filled Fermi sea via $\sqrt{\pi}:\hat{\rho}: = d\hat{\theta}/dx$ and $\sqrt{\pi}:\hat{J}: = d\hat{\phi}/dx$, where $:\cdots:$ denotes normal ordering with respect to the homogeneous ground state $|0\rangle_{\rho_0=0}$. These satisfy the commutation relations $[:\hat{\rho}(x):, :\hat{J}(x'):] = -(i/\pi)(d/dx)\times \delta(x - x')$. Via the axial anomaly, the static chemical potential in Eq. (3) writes an arbitrary density profile into $|0\rangle_{\rho_0}$,

$${}_{\rho_0}\langle 0|:\hat{\rho}(x):|0\rangle_{\rho_0} = \rho_0(x), \qquad {}_{\rho_0}\langle 0|:\hat{J}(x):|0\rangle_{\rho_0} = 0. \tag{4}$$

We perform the quench at time $t = 0$. The dynamics for $t > 0$ are generated by the translationally invariant, "final state" Hamiltonian H_f, which favors a gapped, Mott insulating ground state. Specifically, H_f is the Hamiltonian of the quantum sine-Gordon model,

$$H_f = \frac{1}{K_f}\int dx\left[\frac{1}{2}\left(\frac{d\hat{\Phi}}{dx}\right)^2 + \frac{1}{2}\left(\frac{d\hat{\Theta}}{dx}\right)^2 + \frac{M}{\pi\alpha}\cos(2\sqrt{4\pi K_f}\hat{\Theta})\right]. \tag{5}$$

In Eq. (5) we have expressed H_f in terms of the canonically rescaled boson variables $\hat{\Phi} \equiv \sqrt{K_f}\hat{\phi}$ and $\hat{\Theta} \equiv \hat{\theta}/\sqrt{K_f}$. The Mott gap-inducing interparticle interactions set the parameters M and K_f. In the context of a Fermi lattice gas at commensurate filling, the "Luttinger parameter" K_f characterizes pure forward scattering, while M gives the strength of backward scattering umklapp interactions; α is a cutoff-dependent length scale. The ground state of H_f is gapped for arbitrarily small M over the regime $0 < K_f < 1/2$, in which the quantum sine-Gordon model is integrable [12]. The solitons and antisolitons of the classical sine-Gordon equation appear as massive Dirac fermions in the quantum version [18]. Solitons repel antisolitons for $1/4 < K_f < 1/2$ and attract them for $0 < K_f < 1/4$; in the latter case, additional bosonic bound states (breathers) appear in the spectrum. We choose to quench to the boundary between these two regimes, where $K_f = \bar{K} \equiv 1/4$. At this special "Luther-Emery" point, the interactions between the quantum solitons switch off, and H_f can be *refermionized* [12] in terms of a massive noninteracting soliton field Ψ,

$$H_f = \frac{1}{\bar{K}}\int dx\Psi^\dagger\left(-i\hat{\sigma}^3\frac{d}{dx} + \bar{M}\hat{\sigma}^2\right)\Psi. \tag{6}$$

In this equation, Ψ is a two-component Dirac fermion that is related to the boson fields in Eq. (5) via the bosonization identity, $\Psi^{(1,2)} \propto \exp[i\sqrt{\pi}(\hat{\Phi} \pm \hat{\Theta})]$; $\hat{\sigma}^{2,3}$ are Pauli matrices in the standard basis. The mass gap $\bar{M}$ in Eq. (6) is a nonuniversal, cutoff-dependent quantity.

It is instructive to rewrite H_i [Eq. (3)] in terms of Ψ,

$$H_i = \int dx\left\{\tilde{v}\Psi^\dagger\left(-i\hat{\sigma}^3\frac{d}{dx}\right)\Psi - \frac{\rho_0(x)}{2q}\Psi^\dagger\Psi + \frac{\pi\tilde{v}}{2K^2}[\bar{K}^2 - K^2]:\Psi^\dagger\Psi::\Psi^\dagger\Psi:\right\}, \tag{7}$$

where $\tilde{v} \equiv Kv/\bar{K}$. Comparing Eqs. (6) and (7), we see that the quench with $K = \bar{K}$ is special. For this case only ("noninteracting" quench), the quasiparticles of the initial and final Hamiltonians are in one-to-one correspondence. At any other value of $K \neq \bar{K}$ ("interacting quench"), an elementary excitation of the initial state carries a fraction of the final state quasiparticle number; that is, the "quasiparticle" excitations of the initial LL phase carry $K/\bar{K} = 4K$ of the global $U(1)$ Ψ fermion number charge [16]. When viewed in terms of Ψ, the transition between H_i and H_f permits a dual interpretation as a LL to band insulator quench. Correlation functions in the homogeneous quench $[\rho_0(x) = 0]$ have been previously studied in Refs. [8,13,14].

To characterize the postquench dynamics, we consider the expectation values of the particle number (ρ), kinetic ($\mathcal{K}$) and potential ($\mathcal{U}$) energy densities (the latter two observables are defined with respect to H_f):

$$\rho(t, x) = (1/2)_{\rho_0}\langle 0|{:}\Psi^\dagger(t, x)\Psi(t, x){:}|0\rangle_{\rho_0}, \tag{8a}$$

$$\mathcal{K}(t, x) \equiv -(i/2)_{\rho_0}\langle 0|\Psi^\dagger(t, x)\hat{\sigma}^3\overleftrightarrow{\partial}_x\Psi(t, x)|0\rangle_{\rho_0}, \tag{8b}$$

$$\mathcal{U}(t, x) \equiv {}_{\rho_0}\langle 0|\Psi^\dagger(t, x)\hat{\sigma}^2\Psi(t, x)|0\rangle_{\rho_0}, \tag{8c}$$

where $f\overleftrightarrow{\partial}g \equiv f\partial g - (\partial f)g$. In these equations, $\Psi(t, x)$ denotes the Heisenberg picture fermion operator whose dynamics are generated by H_f in Eq. (6). $\mathcal{U}$ gives the expectation of the cosine operator in the sine-Gordon model [Eq. (5)], and can be interpreted as a (squared) order parameter for the Mott phase. We compute ρ, $\mathcal{K}$, and $\mathcal{U}$ by solving the Heisenberg equations of motion for $\Psi(t, x)$ in terms of the Schrödinger picture components $\Psi^{(1,2)}(0, x)$; the expectation values of products of the latter in the initial state $|0\rangle_{\rho_0}$ are obtained via the bosonization mapping [12]. Exact results for ρ, $\mathcal{K}$, and $\mathcal{U}$ at any time $t \geq 0$ will appear elsewhere [19].

The postquench observables in Eq. (8) depend upon $\rho_0(x)$, $\bar{M}$, and the exponent σ defined via Eq. (2). The noninteracting quench with $K = \bar{K}$ has $\sigma = 0$, while the interacting quench ($K \neq \bar{K}$) has $\sigma > 0$. We confine ourselves to the range $0 \leq \sigma < 1$, for which the $\rho_0(x)$-dependent contributions to ρ, $\mathcal{K}$, and $\mathcal{U}$ are given by ultraviolet (UV) convergent integrals [19]. At $\sigma = 1$, these acquire logarithmic UV divergences, suggesting the onset of a sensitive dependence to lattice scale details.

We now describe our main results, which concern the $\rho_0(x)$-dependent contributions to ρ, $\mathcal{K}$, and $\mathcal{U}$; the behavior of $\mathcal{K}$ and $\mathcal{U}$ for the homogeneous quench $\rho_0 = \rho(t, x) = 0$ will be discussed elsewhere [19]. The exact leading asymptotic expression for $\rho(t, x)$ in the limit $t \to \infty$ was already given by Eq. (1), above. Let us specialize this result to a localized initial density profile. The interacting ($\sigma > 0$) versus noninteracting ($\sigma = 0$) quenches yield qualitatively different behaviors. For the interacting quench, Eq. (1) implies that $\rho(t, x)$ develops a nondispersive response to the initial condition for any $0 < \sigma < 1$. For example, a Gaussian density bump, $\sqrt{\pi}\Delta\rho_0(x) = Q\exp(-x^2/\Delta^2)$, induces the following asymptotic space-time evolution for $t \gg 1/\bar{M}$:

$$\begin{aligned}\rho(t, x) = {}& \frac{Q}{2\sqrt{\pi}\Delta}e^{-[(x-t')^2/\Delta^2]} \\ & - \frac{Q}{2\Delta}\frac{\Gamma(1-\sigma)}{\Gamma(\frac{1+\sigma}{2})}\left[\frac{(K\bar{M}\alpha)^2 t'}{\sqrt{2}\Delta}\right]^{\sigma/2} F_\sigma\left(\frac{x-t'}{\Delta}\right) \\ & + \{x \to -x\},\end{aligned} \tag{9}$$

where $F_\sigma(z) \equiv \exp(-z^2/2)D_{\sigma/2}(\sqrt{2}z)$, $D_\nu(x)$ denotes the parabolic cylinder function, $t' = t/\bar{K}$, and we have written out the explicit form of the prefactor $\mathcal{A}_\sigma$, which is nonuniversal for $\sigma > 0$ and depends upon $\bar{M}\alpha$. The naive continuum calculation gives $\bar{M}\alpha = 15/16$. The divergence of the prefactor at $\sigma = 1$ indicates the onset of sensitivity to the UV sector of the theory.

Equation (9) implies that an antecedent Gaussian density bump splits into right- and left-moving nondispersive waves, for generic Q, Δ, and $K \neq \bar{K}$ ($\sigma > 0$). In the long time limit, the leading response is *strictly linear* in Q, with an amplitude that grows as $t'^{\sigma/2}$. Two Gaussian bumps initially separated by a distance $d \gg \Delta$ can be used to create left- and right-moving waves which pass through each other without changing their form [19]. We dub these rigid, noninteracting density waves "supersolitons" to distinguish them from the elementary quantum solitons annihilated by the fermion field Ψ. We have confirmed the asymptotic result in Eq. (9) by comparing to numerical integration of the exact bosonization expression for ρ. The supersoliton is exhibited in Fig. 2.

Although the precise shape of the supersoliton implied by Eq. (9) deforms continuously with σ, it exhibits the same positive-negative "dipolar" peak profile for any $0 < \sigma < 1$ (see Fig. 2). The negative density dip represents a local evacuation of the filled Fermi sea, which is infinitely deep in the Luttinger model [12]. For any $\sigma > 0$, the integral of the second term in Eq. (9) over real x vanishes, consistent with particle number conservation. In the limit of the

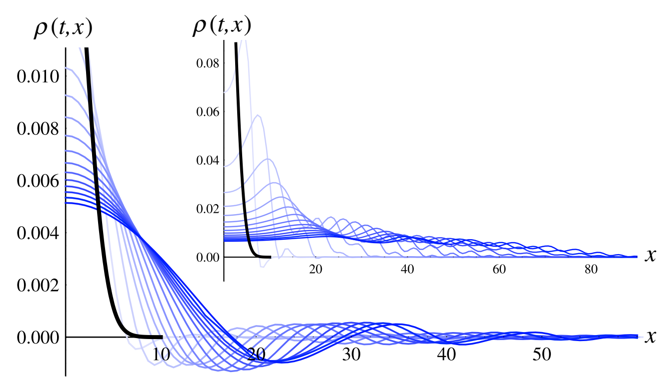

FIG. 3 (color online). The number density evolution as in Fig. 2, but for the noninteracting quench $K = \bar{K}$ ($\sigma = 0$). The initial bump (heavy black line) has area $Q = 0.1$ in the main figure and $Q = 1$ in the inset; in both cases $\Delta = 3$. The evolution is reflection symmetric about $x = 0$. Now there is no fractionalization of the initial LL quasiparticles with respect to the insulator and, consequently, the dynamics are simply dispersive with no supersolitons or inhomogeneity growth.

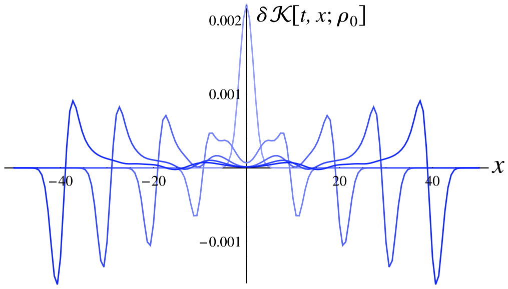

FIG. 4 (color online). The kinetic energy density supersolitons. This figure depicts the postquench space-time evolution of the relative kinetic energy density expectation value $\delta\mathcal{K}[t,x;\rho_0]$ (see text) for $K = 0.77 \neq \bar{K}$ and an initial Gaussian density bump.

noninteracting quench $\sigma \to 0$, the right-hand side of Eq. (9) vanishes; in this case, the response obtains entirely from subleading terms that do not grow with t (and conserve the particle number), but which we have not written here. The same is true in Eq. (1) because $\mathcal{A}_\sigma \to 1$ when $\sigma \to 0$.

Figure 3 depicts the number density $\rho(t,x)$ for the case $\sigma = 0$, obtained by numerical integration of the exact result. The main message of this figure is that the noninteracting postquench dynamics are "passive" and dispersive, depending sensitively upon the details of the initial inhomogeneity and showing no amplification.

In the interacting quench, the supersoliton is also observed in the relative kinetic energy density, defined as $\delta\mathcal{K}[t,x;\rho_0] \equiv \mathcal{K}[t,x;\rho_0] - \mathcal{K}[t,x;0]$, shown in Fig. 4. By contrast, we find that the potential energy density $\mathcal{U}(t,x)$ does not exhibit the supersoliton on top of the homogeneous background it acquires after the quench. The amplification in Eq. (1) does not therefore appear related to a Kibble-Zurek process [5] in the order parameter.

We interpret the growth mechanism in Eqs. (1) and (9) by analogy to the equilibrium tunneling density of states (TDOS) $\nu(\omega)$ in a LL [16]. Upon tunneling into a one channel quantum wire with Luttinger parameter K, the conductance at a bias $\omega = eV$ diminishes as $\nu(\omega) \sim |\omega|^\sigma$, where σ is defined as in Eq. (2), but with $\bar{K} = 1$. In the limit $\omega \to 0$, $\nu(\omega)$ vanishes because the fractionalization of a "whole" electron into LL "quasiparticles" with charge Ke is prohibited by phase space restrictions [16]. In the quench studied here, the evolution due to the massive final state Hamiltonian H_f can be viewed as a spectroscopy of the initial LL state; the analog of the frequency ω in the TDOS is the evolution interval $\bar{M}^2 t$. We might therefore anticipate $\rho(t,x) \sim t^\sigma$, with σ defined by Eq. (2). That the leading power is $\sigma/2$ in Eqs. (1) and (9) results from a cancelation of t^σ terms.

In a lattice model realization of the quench (see Ref. [19] for an example), the supersoliton growth is cut off at a time scale of order $t_c \sim 1/\bar{M}^2 a$, where a denotes the lattice spacing. The dynamics become sensitive to model details (i.e., irrelevant operators) for $t \gtrsim t_c$. Any real system will ultimately thermalize due to interactions with its environment and deviations from integrability.

In conclusion, we have shown that a quantum quench can beget a strongly inhomogeneous state, due to the interplay between quasiparticle fractionalization and the presence of a mass scale in the final state Hamiltonian. Fractionalization is a robust feature of 1D gapless phases, so we expect the inhomogeneity proliferation to occur in many 1D quantum quenches. It would be interesting to consider quenches to final states away from the free fermion LE point where (super?) soliton-soliton interactions can play a role in the dynamics.

We thank Leon Balents for helpful discussions of LL physics. This work was supported by the National Science Foundation under Grant No. DMR-0547769 and by the David and Lucile Packard Foundation.

*psiborf@rci.rutgers.edu

[1] I. Bloch, J. Dalibard, and W. Zwerger, Rev. Mod. Phys. **80**, 885 (2008).
[2] T. Kinoshita, T. Wenger, and D. S. Weiss, Nature (London) **440**, 900 (2006).
[3] L. E. Sadler *et al.*, Nature (London) **443**, 312 (2006).
[4] M. Greiner *et al.*, Nature (London) **419**, 51 (2002).
[5] T. W. B. Kibble, J. Phys. A **9**, 1387 (1976); W. H. Zurek, Nature (London) **317**, 505 (1985).
[6] M. Rigol *et al.*, Phys. Rev. Lett. **98**, 050405 (2007); M. Rigol, V. Dunjko, and M. Olshanii, Nature (London) **452**, 854 (2008).
[7] P. Calabrese and J. Cardy, Phys. Rev. Lett. **96**, 136801 (2006); J. Stat. Mech. (2007) P06008.
[8] V. Gritsev *et al.*, Phys. Rev. Lett. **99**, 200404 (2007).
[9] D. Rossini *et al.*, Phys. Rev. Lett. **102**, 127204 (2009).
[10] C. De Grandi, V. Gritsev, and A. Polkovnikov, Phys. Rev. B **81**, 012303 (2010); **81**, 224301 (2010).
[11] M. Dzero, E. A. Yuzbashyan, and B. L. Altshuler, Europhys. Lett. **85**, 20 004 (2009).
[12] For a review, see, e.g., T. Giamarchi, *Quantum Physics in One Dimension* (Oxford University Press, Oxford, 2004).
[13] M. A. Cazalilla, Phys. Rev. Lett. **97**, 156403 (2006); A. Iucci and M. A. Cazalilla, Phys. Rev. A **80**, 063619 (2009); New J. Phys. **12**, 055019 (2010).
[14] J. Sabio and S. Kehrein, New J. Phys. **12**, 055008 (2010); P. Barmettler *et al.*, *ibid.* **12**, 055017 (2010).
[15] J. Mossel and J.-S. Caux, New J. Phys. **12**, 055028 (2010); J. Lancaster and A. Mitra, Phys. Rev. E **81**, 061134 (2010).
[16] For a review, see M. P. A. Fisher and L. I. Glazman, in *Mesoscopic Electron Transport*, edited by Sohn, Kouwenhoven, and Schön (Kluwer, The Netherlands, 1997).
[17] M. A. Cazalilla, J. Phys. B **37**, S1 (2004).
[18] For a review, see, e.g., R. Rajaraman, *Solitons and Instantons* (North-Holland, Amsterdam, 1982).
[19] M. S. Foster, E. A. Yuzbashyan, and B. L. Altshuler (to be published).